CrossMark

Wettability and Reactivity of ZrB$_2$ Substrates with Liquid Al

R. Nowak, N. Sobczak, G. Bruzda, J. Wojewoda-Budka, L. Litynska-Dobrzynska, M. Homa, I. Kaban, L. Xi, and L. Jaworska

(Submitted December 9, 2015; published online January 28, 2016)

Wetting characteristics of the Al/ZrB$_2$ system were experimentally determined by the sessile drop method with application of separate heating of the ZrB$_2$ and Al samples and combined with in situ cleaning of Al drop from native oxide film directly in vacuum chamber. The tests were performed in ultrahigh vacuum of 10^{-6} mbar at temperatures 710, 800, and 900 °C as well as in flowing inert gas (Ar) atmosphere at 1400 °C. The results evidenced that liquid Al does not wet ZrB$_2$ substrate at 710 and 800 °C, forming high contact angles (θ) of 128° and 120°, respectively. At 900 °C, wetting phenomenon ($\theta < 90°$) occurs in 29th minute and the contact angle decreases monotonically to the final value of 80°. At 1400 °C, wetting takes place immediately after drop deposition with a fast decrease in the contact angle to 76°. The solidified Al/ZrB$_2$ couples were studied by scanning and transmission electron microscopy coupled with x-ray energy diffraction spectroscopy. Structural characterization revealed that only in the Al/ZrB$_2$ couple produced at the highest temperature of 1400 °C new phases (Al$_3$Zr, AlB$_2$ and α-Al$_2$O$_3$) were formed.

Keywords	Al-ZrB$_2$, high-temperature reactivity, wettability

1. Introduction

Zirconium diboride ZrB$_2$ belongs to a family of transition metals borides known as Ultra-High-Temperature Ceramics (UHTCs) (Ref 1). It has extremely high melting temperature, high thermal and electrical conductivity, excellent thermal shock resistance, high hardness and chemical inertness. Such unique combination of thermophysical, mechanical, and utility properties makes ZrB$_2$-based ceramics suitable for the extreme thermal and chemically aggressive environments (Ref 2). Therefore, this class of materials has received much attention to explore for wide applications in many structures and components by synthesis of metal-ceramic composites and by means of joining to metals or other ceramics. Recently, attempts have been done to produce Al-ZrB$_2$ metal matrix composites by different techniques, among which liquid-assisted ones are the most promising (Ref 3, 4). Thus, a comprehensive knowledge concerning wetting behavior and reactivity in the Al/ZrB$_2$ system is of great practical importance.

It should be mentioned that the literature data correspond to the results of wetting experiments performed on ZrB$_2$ substrates produced using sintering aids whose type and amount are often overlooked. That makes difficult an understanding of the factors affecting wetting behavior and reactivity of the system. It is also one of the reasons of the large scattering and even contradicting of experimental data as shown in Fig. 1 for the works (Ref 5-11). For example, Samsonov et al. (Ref 7) reported that aluminum forms a contact angle of 106° on the ZrB$_2$ substrate at 900 °C in vacuum. Similar contact angle ($\theta = 107°$) was recorded by Yasinskaya (Ref 8) in helium but at higher temperature of 1000 °C, while Achmatov et al. (Ref 9) obtained almost one and half times larger value ($\theta = 151°$) for the same temperature, atmosphere and measuring time. On the other hand, Kennedy and Karantzalis (Ref 13) reported that the ZrB$_2$ particles were ready incorporated in Al melt thus allowing to produce homogeneous Al-ZrB$_2$ slurry and uniform distribution of the ZrB$_2$ particles in cast composite produced at temperatures similar to those reported in wettability studies (Ref 7-9). Kennedy and Karantzalis (Ref 13) suggested that the results obtained in their trials present an experimental evidence of a good wetting between liquid Al and ZrB$_2$, i.e., the contact angle in the system should be $\theta \ll 90°$ and it is related with metal-like character of ZrB$_2$.

Among numerous factors affecting wetting properties of metal/ceramic systems discussed in the works (Ref 14-18), for experimental data reported for the Al/ZrB$_2$ system (Ref 5-11), two factors seem to have the strongest effect on the contact angle measurements:

(1) the presence of native oxide film on the Al drop, since all results were produced using classical contact heating procedure;

R. Nowak, G. Bruzda, and **M. Homa**, Foundry Research Institute, 73 Zakopianska St., 30-418 Cracow, Poland; **N. Sobczak**, Foundry Research Institute, 73 Zakopianska St., 30-418 Cracow, Poland; and Motor Transport Institute, 80 Jagiellonska St., 03-301 Warsaw, Poland; **J. Wojewoda-Budka** and **L. Litynska-Dobrzynska**, Institute of Metallurgy and Materials Science, Polish Academy of Sciences, 25 Reymonta St., 30-059 Cracow, Poland; **I. Kaban**, IFW Dresden, Institute for Complex Materials, Helmholtzstr. 20, 01069 Dresden, Germany; **L. Xi**, IFW Dresden, Institute for Complex Materials, Helmholtzstr. 20, 01069 Dresden, Germany; and TU Dresden, Institute of Materials Science, 01062 Dresden, Germany; and **L. Jaworska**, Institute of Advanced Manufacturing Technology, 37A Wroclawska St., 30-011 Cracow, Poland. Contact e-mail: rafal.nowak@iod.krakow.pl.

(2) the chemistry of the ZrB_2 substrate affected by chemical composition of starting ZrB_2 powder and sintering aids used for the production of dense ZrB_2 ceramic.

In this study, the above two factors have been eliminated by application of an improved testing procedure of wettability studies allowing to produce oxide-free Al drops directly in vacuum chamber and using dense polycrystalline ZrB_2 substrates free of sintering aids. The paper focuses on experimental investigation of the effect of temperature on the relationship between wetting behavior and reactivity in the Al/ZrB_2 couples by detailed structural characterization of interfaces using scanning and transmission electron microscopy techniques.

2. Experimental Procedure

The wetting behavior of polycrystalline ZrB_2 substrates by liquid aluminum (99.999%) was examined by the sessile drop method at the temperatures of 710, 800, 900, 1400 °C for 120, 120, 60, and 15 min, respectively. For temperatures up to 900 °C, the tests were carried out under ultrahigh vacuum, while the test at the highest temperature of 1400 °C was performed in flowing inert gas (Ar) in order to prevent evaporation of Al. The wettability tests were performed in experimental complex for investigations of high-temperature phenomena described in details in the work (Ref [19]). The capillary purification (CP) procedure comprising of squeezing of the Al drops from the alumina capillary was applied in order to remove the primary native oxide film from the aluminum sample as well as to avoid the effect of heating history by non-contact heating of both reactants (Ref [14]).

The ZrB_2 substrates were prepared from 5 μm powder of 99% purity from US Research Nanomaterials, Inc (Zr—80.03; B—18.97; N < 0.08%; Si < 0.1; Fe < 0.07; Ni < 0.05, wt.%) by high-temperature high-pressure sintering at 1883 °C under 5 GPa pressure for 25 s using experimental facility of the Institute of Advanced Manufacturing Technology, Cracow. The density of the ZrB_2 substrates was equal to 94 % of the theoretical density and the surface roughness was $R_a = 420$ nm. During the wettability tests, the images of drop/substrate couples were recorded by means of high-speed high-resolution camera MC1310 with a rate of 100 frames per second (fps) during squeezing metal and 10 fps during isothermal heating and cooling up to solidification temperature. The collected images were used for estimation of the contact angle values (θ) with a special software ASTRA2 (IENI-CNR, Italy (Ref [20], [21])) as well as for making a real-time movie of high-temperature test (SUPPLEMENTARY Data 1-4).

The sessile drop couples after wettability tests were studied by scanning electron microscope (SEM) equipped with energy-dispersive x-ray spectroscopy (EDS) analyser. The detailed structural characterization of selected cross-sectioned samples was undertaken using transmission electron microscope TECNAI G2 FEG super TWIN (200 kV) equipped with high angle annular dark field (HAADF) detector and EDAX energy dispersive x-ray spectroscopy (EDS) system. The thin foils for the TEM studies taken from particular locations were produced using FEI Quanta 3D focused ion beam (FIB) instrument.

3. Results and Discussion

The contact angle values of obtained in the present wettability tests for Al/ZrB_2 couples are presented in Fig. 1, whereas the real-time experiments are demonstrated by the movies placed in Supplement 1. At temperatures of 710 and 800 °C, liquid Al did not wet the ZrB_2 substrate. At 710 °C, the contact angle was almost constant for 120 min test showing the final value of $\theta_f^{710} = 128°$. For the 800 °C test, the contact angle slightly decreased for the first 20 min after drop deposition and reached the value of $\theta_f^{800} = 120°$.

At the beginning of the test at 900 °C, aluminum did not wet ZrB_2 forming $\theta = 129°$, but the contact angle continuously decreased. The transition from non-wetting-to-wetting ($\theta = 90°$) was observed after about 29 min, and the contact angle reached the final value of $\theta_f^{900} = 80°$ in 60th min. In opposite to the above observations, the test performed at 1400 °C revealed wetting of ZrB_2 by liquid Al immediately
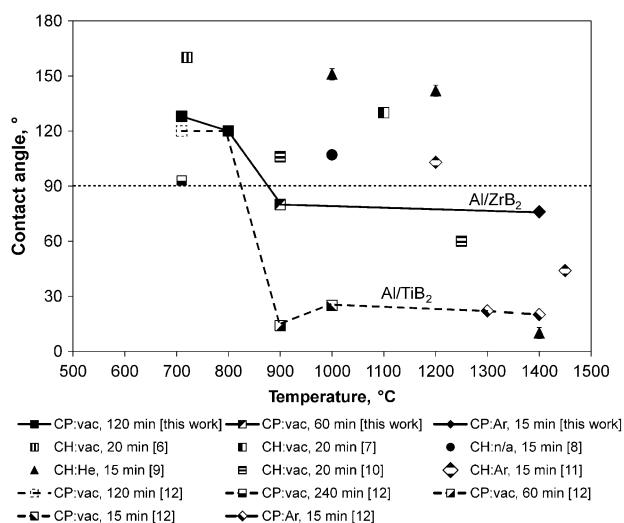

Fig. 1 Experimental data on the effect of temperature and testing conditions on wetting properties of Al/ZrB_2 system (Ref [6-11]), compared to Al/TiB_2 (Ref [12])
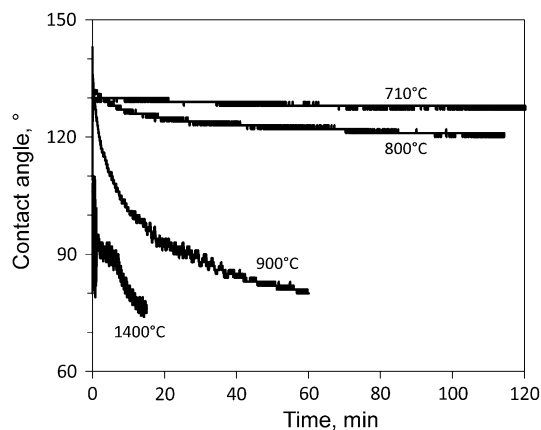

Fig. 2 The effect of temperature on wetting kinetics of liquid Al on ZrB_2 substrate recordered by the sessile drop method using capillary purification technique

after drop deposition, followed by a fast decrease in the contact angle to a value of $\theta_f^{1400} = 76°$ after 15 min (Fig. 2).

Following to the classification of the wetting types proposed by Eustathopoulos (Ref 22), it can be concluded from the shape of the wetting kinetics curves (Fig. 2) that the wetting in the Al/ZrB$_2$ system at 900 and 1400 °C has reactive character. To identify the mechanism responsible for the reactive wetting, the surfaces and the cross sections of the solidified Al/ZrB$_2$ couples were examined by SEM and EDS techniques (Fig. 3). It has to be mentioned that in EDS technique, simultaneous analysis of light elements such as boron and heavy elements such as zircon is very difficult. At high acceleration voltages of the primary electron beam, the peaks from B merge with those from C, while at low acceleration voltages, the peaks from Zr are too weak. Therefore, in this study, the EDS analysis was used only for a qualitative characterization of the solidified Al/ZrB$_2$ couples. The SEM/EDS analysis made on the cross-sectioned samples under magnifications up to 10000× did not show reactivity between liquid Al and ZrB$_2$ at 710 °C. There was no evidence of any reaction product neither under the drop nor outside the drop (Fig. 3a).

Similar results were obtained for the sessile drop couple produced at 800 °C (Fig. 3b). Moreover, despite a good wetting, SEM/EDS analysis did not reveal any significant differences in the couple produced at 900 °C (Fig. 3c). Its TEM characterization also showed the absence of the reactively formed phases. But in this case, liquid metal penetration along the grain boundaries in the ZrB$_2$ substrate was well distinguished, particularly using black field (BF) observation (Fig. 3d).

In contrast to the low-temperature experiments, a strong reactivity between liquid Al and ZrB$_2$ ceramic took place at 1400 °C. SEM/EDS analysis of the top-view (Fig. 4a-c) couple showed reactively changed surfaces of the drop and of the ZrB$_2$ substrate. As illustrated in Fig. 4a, b, the first area around the drop represents spreading halo on the substrates and consists of numerous precipitates of a light contrast showing its dendrite-like growth with smooth transition to the next ring of a darker contrast placed beyond the area revealed in Fig. 4c. Both of these features arose due to the reaction at the liquid Al/substrate (light area) and the aluminum vapor/substrate (dark ring) interfaces, respectively. Further observations under higher magnification brought an additional information on the three types of particles, which are well distinguished in the light area: (1) large needle-like precipitates of gray color, (2) hexagonal plate-like crystals of white color and (3) dark precipitates.

From comparison of the chemical compositions of the selected precipitates and analysis of the Al-Zr and Al-B (Ref 23) phase equilibrium diagrams, it can be deduced that the large needles containing Al and Zr represent Al$_3$Zr phase. The hexagonal plate-like crystals surrounding Al$_3$Zr needles are enriched in zirconium. Their shape and location on the surface of the solidified metal layer extending outside the drop suggest that it is ZrB$_2$ formed from Zr- and B-saturated melt during cooling by dissolution-precipitation mechanism. EDS analysis of the dark particles contains aluminum and oxygen; thus one may conclude that they represent alumina. SEM observation of the cross-sectioned sample (Fig. 4d-f) shows that spreading halo layer growing outside the drop (Fig. 4d) is composed of
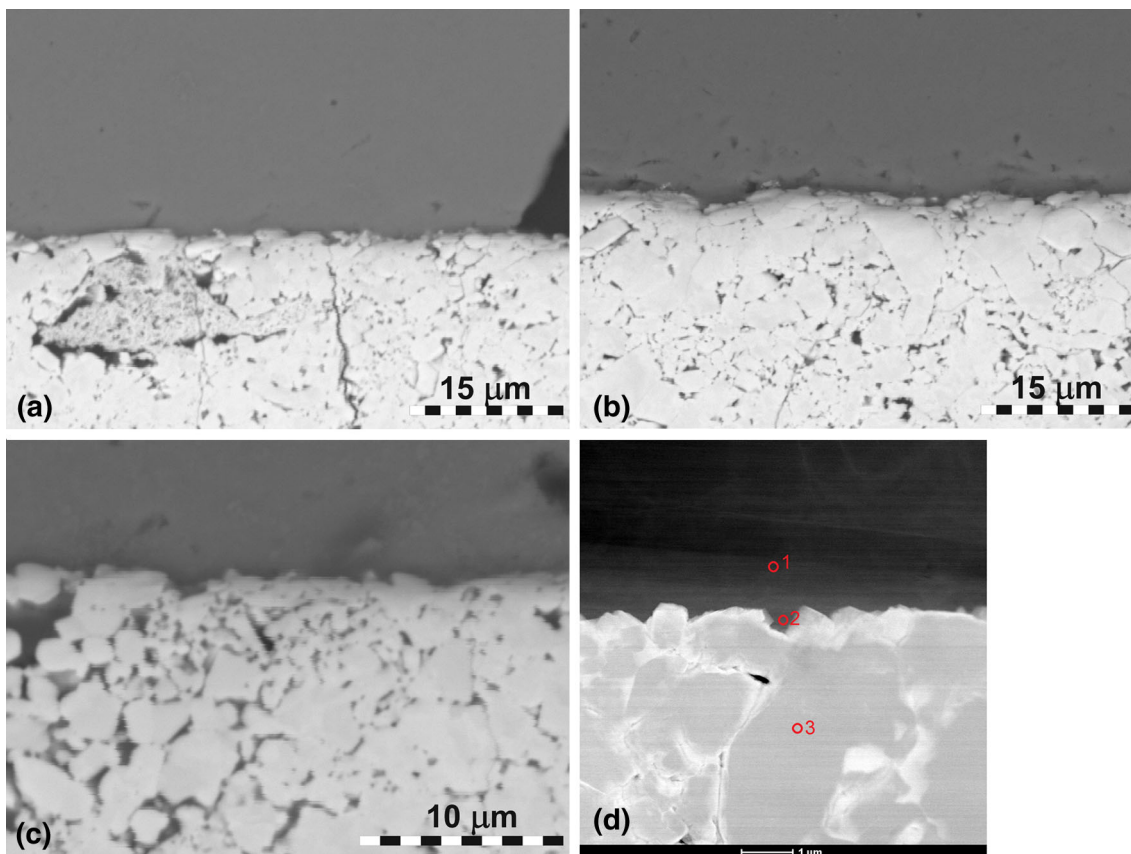

Fig. 3 Microstructure of cross-sectioned Al/ZrB$_2$ couples after wettability tests at different temperatures: (a) 710 °C, (b) 800 °C and (c, d) 900 °C; (a-c) SEM images; (d) TEM BF image
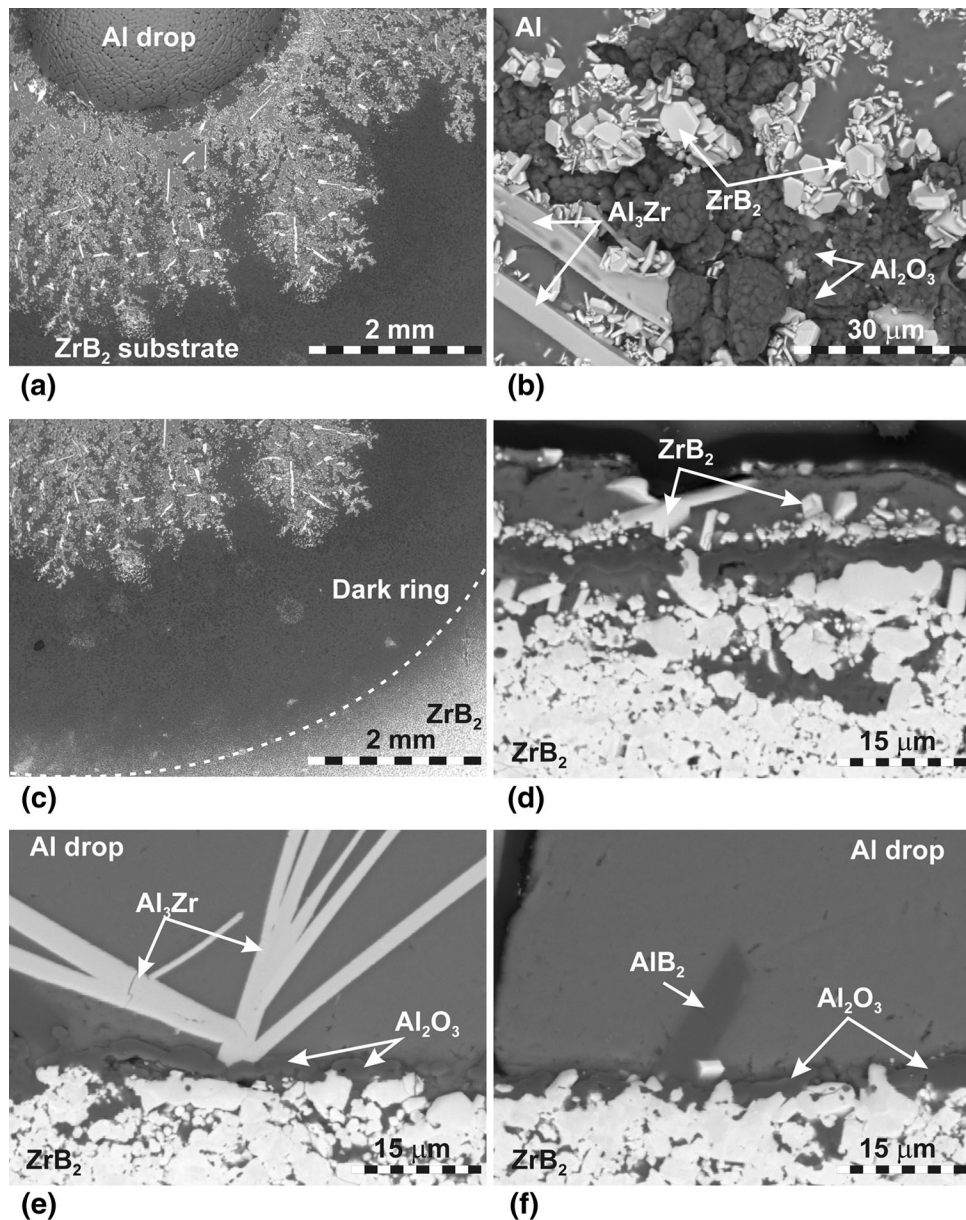
Fig. 4 SEM top-view (a-c) and cross section (d-f) images of the Al/ZrB$_2$ couple (1400 °C): (a) spreading halo next to the Al drop; (b) higher magnification of (a) with visible precipitates formed due to high-temperature interaction between liquid Al and ZrB$_2$ substrate: Al$_3$Zr—needles, ZrB$_2$—hexagonal plate-like crystals, Al$_2$O$_3$—dark precipitates; (c) dark ring surrounding spreading halo region; (d) structure of the spreading halo layer outside the drop showing separate ZrB$_2$ crystals; (e) needle-like Al$_3$Zr precipitates formed at the drop-side interface; (f) block AlB$_2$ crystal and thin layer of Al$_2$O$_3$

metallic matrix and numerous small Al$_3$Zr needles and AlB$_2$ particles. Their well-distinguished regular shape and specific location far from the interface suggest that they are formed by another mechanism. These precipitates rather nucleated from the liquid saturated with boron and zirconium during cooling by dissolution-precipitation.

SEM/EDS characterization of the cross-sectioned couple produced at 1400 °C (Fig. 4e, f) also evidenced the presence of new phases reactively formed at the interface directly under the drop. The large needles of about 80 μm in length, identified as Al$_3$Zr compound (Fig. 4e), are present occasionally at the interface. They do not form continuous interfacial layer, but they were nucleated at the interface and grow inside the drop. The presence of Al$_3$Zr needles is accompanied by the blocky

crystals of AlB$_2$ also nucleated at the interface and growing inside the drop (Fig. 4f). From the above observations, one may conclude that the following redox reaction may take place at the Al/ZrB$_2$ interface:

$$4Al + ZrB_2 = AlB_2 + Al_3Zr \qquad (Eq\ 1)$$
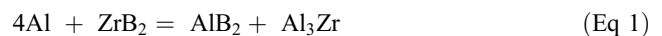
The TEM observations under high magnification (Fig. 5a, b) combined with EDS analysis (Fig. 5c) of cross-sectioned drop reveal that in the vicinity of the Al$_3$Zr and AlB$_2$ precipitates at the interface, dark crystals form discontinuous thin layer (Fig. 5b). The maps of elements distribution (Fig. 5c) allow to identify that the above layer is composed of densely packed particles containing aluminum and oxygen. Occasionally, the layer is intermixed with the particles of regular shape and rich
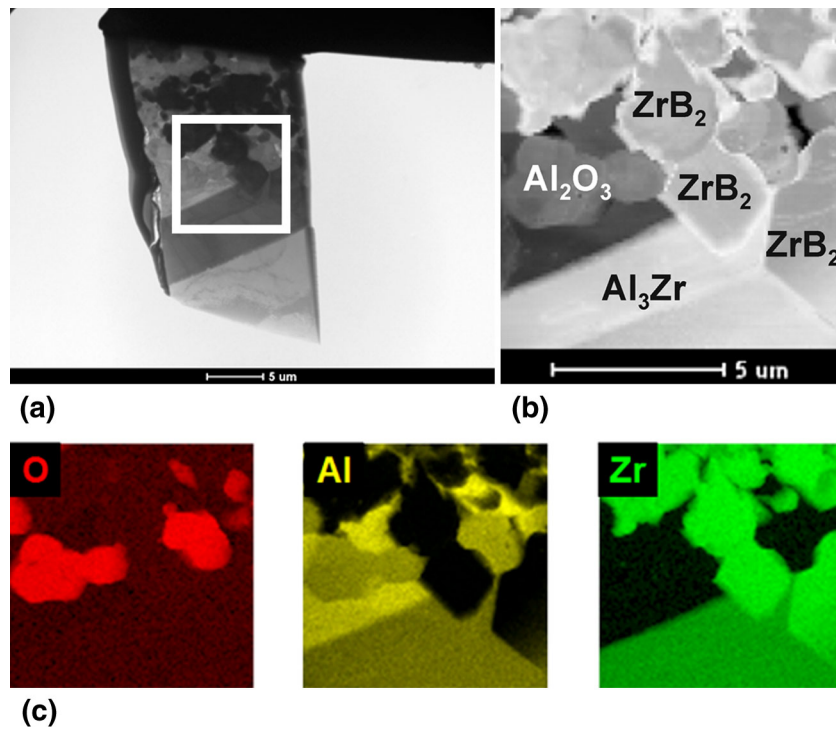
Fig. 5 (a, b) TEM images of cross-sectioned Al/ZrB$_2$ couple (1400 °C) with marked place for FIB cutting of thin foil for TEM characterization: (a) overview; (b) BF image of the marked area and (c) corresponding maps of elements distribution

in Zr. Thus, it was concluded that this layer is mostly composed of alumina precipitates, while Zr-rich particles that represent ZrB$_2$ phase are similar to those noted in the top-view observations in Fig. 4(b). The reason for the formation of alumina in Al/ZrB$_2$ couples is related with the presence of ZrO$_2$ phase that is unavoidable in ZrB$_2$-based ceramics (Ref 1, 3, 5). As it was recently reported by Sobczak et al. (Ref 24), at high temperature liquid aluminum reduces ZrO$_2$ to form Al$_2$O$_3$ and either Zr or Al$_3$Zr according to following redox reactions:

$$4Al \ + \ 3ZrO_2 \ = \ 2Al_2O_3 \ + \ 3Zr \qquad (Eq\ 2)$$

$$13Al \ + \ 3ZrO_2 \ = \ 3Al_3Zr \ + \ 2Al_2O_3 \qquad (Eq\ 3)$$
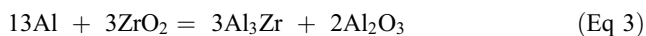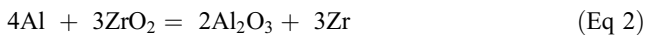
The above observations on the occurrence of redox reactions are in a good agreement with those evidenced by Xi et al. in another Al/metal boride system such as Al/TiB$_2$ (Ref 12). These reactively formed oxide particles as the seeds for heterogeneous nucleation may affect further formation and growth of ZrB$_2$ crystals. The last statement has been proved by detailed TEM analysis of the region shown in Fig. 5(b) and the analysis of the selected area electron diffraction (SAED) patterns taken from all the specific places. Large needles visible in both bright field images were identified as a tetragonal Al$_3$Zr phase, below which the aluminum was present. The bright field image in Figure 6 shows the hexagonal ZrB$_2$ crystals and α-Al$_2$O$_3$ particles which location suggests that the ZrB$_2$ phase nucleates at the surface of alumina and it grows surrounding Al$_2$O$_3$ particles. Similar effect of oxide particles as the seeds for heterogeneous nucleation of metal boride HfB$_2$ precipitates from Hf- and B-saturated melt was reported by Passerone et al. for the Ni/HfB$_2$ couples and explained by dissolution-precipitation mechanism (Ref 25).

Our observations for the Al/ZrB$_2$ couples differ from existing reports on the strong dissolutive wetting mechanism in the Ni/boride systems, in which good wetting ($\theta < 10°$ in Ni/ZrB$_2$ (Ref 26), 46° in Ni/TiB$_2$ (Ref 27) and 18° in Ni/HfB$_2$ (Ref 25)) was accompanied with the formation of a deep crater in the substrate under the drop. The absence of a crater in the Al/ZrB$_2$ can be explained, at least partly, by much lower solubility of Zr and B in liquid Al (~0.3 at.% Zr and ~0.6 at.% B at 900 °C and ~1 at.% Zr and ~2 at.% B at 1000 °C) (Ref 23, 28, 29) compared to Zr, Ti, Hf, and B in liquid Ni (~90 at.% Zr, 45 at.% Hf, 92 at.% Ti and ~58 at.% B at 1500 °C) (Ref 23, 30-32). Good wetting without formation of a crater as well as interfacial reaction products was observed in the Al/TiB$_2$ couples (Fig. 1) (Ref 12), also characterized by low solubility of Ti and B in liquid Al (~0.73 at.% Ti and ~0.6 at.% B at 900 °C) (Ref 28, 29). Moreover, both the Al-Zr and Al-Ti belong to the peritectic-type systems Al-Me, in which at peritectic temperature, the solubility of Me in Al is even lower in liquid state compared to that in solid state (Ref 23).

Comparison of the results of this study for the Al/ZrB$_2$ couples and those for the Al/TiB$_2$ ones (Ref 12), both obtained using the same experimental facility and testing procedure (Fig. 1), shows that non-wetting-to-wetting transition takes place in the Al/ZrB$_2$ system at a temperature of about 50 °C bigger than that in the Al/TiB$_2$ system, while the final contact angles formed at 900 and 1400 °C on TiB$_2$ are about 50° to 60° smaller than those on ZrB$_2$. Also in the case of Cu and Au, widely accepted as non-reactive metals, the contact angles formed on ZrB$_2$ [80° and 34°, respectively (Ref 15)] are bigger than those on TiB$_2$ [50° and 15°, respectively (Ref 33)]. Contrary to common opinion on good wetting of transition metal borides by liquid Cu and Au due to the 'metallic-like'
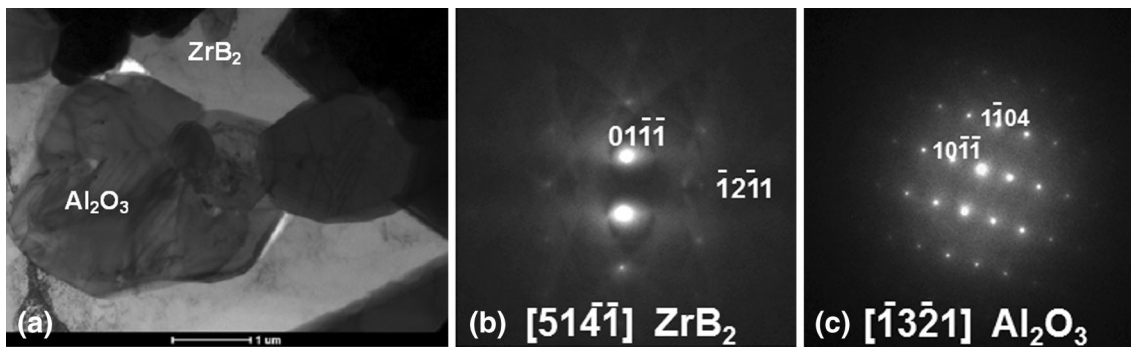
Fig. 6 BF image of the cross-sectioned Al/ZrB$_2$ couple (1400 °C) showing ZrB$_2$ precipitates formed from liquid phase and reactively formed α-Al$_2$O$_3$ particles (a) with corresponding SAED patterns for: (b) ZrB$_2$ and (c) α-Al$_2$O$_3$

character of borides, Aizenshtein et al. (Ref 33) suggested that also the chemical interaction stands behind good wetting in these systems. Aizenshtein et al. explained better wetting in the Au/TiB$_2$ than in the Cu/TiB$_2$ by significantly higher dissolution of TiB$_2$ in liquid Au than in liquid Cu.

For the Al/ZrB$_2$ and the Al/TiB$_2$ systems at 900 and 1400 °C, we also suggest that wetting has reactive character, despite two important facts, i.e., (1) no interfacial reactive products were noted in the Al/ZrB$_2$ and Al/TiB$_2$ couples and their interfaces were smooth after testing at 900 °C, (2) for the 1400 °C test, new interfacial phases (Al$_3$Zr or Al$_3$Ti, AlB$_2$ and α-Al$_2$O$_3$) did not form continuous layers in the triple line area and thus their effect on wetting behavior is negligible. We suggest that significant change in the chemistry of initially pure Al drops in both the Al/ZrB$_2$ and Al/TiB$_2$ couples after testing at 1400 °C is attributed to dissolution of B and Zr (or Ti) from the substrates and it might be reflected to the dominant contribution of dissolutive wetting mechanism . There is also another feature that should be taken into consideration. Following Al-B phase diagram (Ref 29), the AlB$_2$ phase, identified in both couples, cannot exist at 1400 °C but it can be formed during cooling from B-saturated melt by either peritectic or eutectic transformations. Considering an analogy of the Al-Zr-B and Al-Ti-B phase diagrams suggested by Whang et al. (Ref 34), one may expect that similar to the Al-Ti-B system the peritectic reaction takes place in the Al-Zr-B system and it might affect phase transformation in the Al/boride couples during their cooling after wettability tests. Following new data on peritectic temperature in the Al-B-Ti system (877 °C) reported in (Ref 35), one may assume that at the test temperatures of 900 and 1400 °C, the AlB$_{12}$ phase is reactively formed at the Al/TiB$_2$ interface and it is responsible for good wetting of TiB$_2$ by liquid Al drop. However, during cooling when the system reaches the peritectic temperature, this phase reacts with liquid to form a new phase AlB$_2$:

$$AlB_{12} + L \rightarrow AlB_2 + TiB_2 \qquad (Eq\ 4)$$

In such a case, the AlB$_{12}$ phase, formed during wettability test, disappears while the TiB$_2$ phase, freshly formed during cooling by dissolution-precipitation mechanism, nucleates and grows at the TiB$_2$ substrate thus masking previous dissolution of the substrate in liquid drop.

If the analogy of the Al-B-Ti and Al-B-Zr phase diagrams is true, than a good wetting observed in both Al/ZrB$_2$ and Al/TiB$_2$ couples at 900 and 1400 °C is related to the formation of the same interfacial reaction product AlB$_{12}$. But since cooling

history affects the final structure of solidified couples, the real interface structure and topography formed at the test temperature is unseen. It is also true not only for disappearance of AlB$_{12}$ phase in the solidified couples but also for high smoothness of its interfaces. We suggest that re-precipitation of TiB$_2$ or ZrB$_2$ from Ti- or Zr- saturated melts on the boride substrate surface causes the formation of more rough topography of drop-side interface, compared to its initial state. However, as soon as peritectic temperature is reached during cooling, the dissolution of Ti and Zr in Al increases and some amount of corresponding boride, freshly formed by re-precipitation, might be again dissolved in the surrounding solidified drop consequently resulting in more smooth drop-side interface.

4. Conclusions

At low temperatures of 710 and 800 °C, the ZrB$_2$ substrates, sintered from pure ZrB$_2$ powder without aids, show non-wetting behavior in contact with oxide-free liquid Al. Increase in temperature causes non-wetting to wetting transition in the Al/ZrB$_2$ system and formation of final contact angles of 80° and 76° at a temperature of 900 and 1400 °C, respectively.

Analysis of the solidified sessile drop samples with scanning and transition electron microscopy techniques do not show any chemical or structural changes in the Al/ZrB$_2$ couples produced at 710 and 800 °C. Also in the case of the 900 °C test, no interfacial reaction products are noted to occur; however, liquid metal penetration along grain boundaries of the substrate takes place.

On the contrary at 1400 °C, strong interaction of the ZrB$_2$ substrate with both liquid Al and Al vapor, accompanied with substrate dissolution in liquid metal, intensive liquid metal spreading and penetration inside the substrate as well as with the formation of new phases, causes significant changes in the structure and chemistry of Al/ZrB$_2$ couple. The drop-side interface becomes decorated with Al$_3$Zr needles and blocky AlB$_2$ crystals, while its substrate-side is covered with almost continuous layer composed with fine densely packed α-Al$_2$O$_3$ particles separated by or surrounded with ZrB$_2$ phase. These observations show a strong effect of residual oxides in the ZrB$_2$ substrates on high-temperature interaction and the formation of final structure in the Al/ZrB$_2$ couples. At high temperature, liquid Al reduces ZrO$_2$ to form α-Al$_2$O$_3$ particles, which in the next stage play a role of seeds for heterogeneous nucleation of

plate-like hexagonal precipitates of ZrB_2 from B- and Zr-saturated aluminum through the dissolution-precipitation mechanism.

Due to the fact that the interfaces formed in the Al/ZrB_2 couples at 900 and 1400 °C remain smooth, it was suggested that good wetting is related with rather direct interfacial chemical reaction and the formation of wettable AlB_{12} that during cooling is consumed by the possible peritectic reaction $(AlB_{12} + L \rightarrow AlB_2 + ZiB_2)$.

Acknowledgments

Open Access

References

1. E. Wuchina, et al., UHTCs: Ultra-High Temperature Ceramic Materials for Extreme Environment Applications, W.G. Fahrenholtz, E. Wuchina, W.E. Lee, and Y. Zhou Eds., Wiley, New York, 2014
2. J.K. Sonber and A.K. Suri, Synthesis and Consolidation of Zirconium Diboride: Review, *Adv. Appl. Ceram.*, 2011, **110**(6), p 321–334
3. Z. Asadipanah and M. Rajabi, Production of Al–ZrB2 Nano-Composites by Microwave Sintering Process, *J. Mater. Sci.*, 2015, **26**(8), p 6148–6156
4. E. Ghasali, A. Pakseresht, F. Safari-Kooshali, M. Agheli, and T. Ebadzadeh, Investigation on Microstructure and Mechanical Behavior of Al–ZrB₂ Composite Prepared by Microwave and Spark Plasma Sintering, *Mater. Sci. Eng.*, 2015, **627**, p 27–30
5. G.Y. Zhang, W.M. Guo, D.W. Ni, and Y.M. Kan Ultrahigh Temperature Ceramics (UHTCs) Based on ZrB_2 and HfB_2 Systems: Powder Synthesis, Densification and Mechanical Properties, *J. Phys.*, 2009, **176**(1), p 012041, doi:10.1088/1742-6596/176/1/012041
6. A. Merz and H. Kotsch, *Eisenach-Pulverme Metallurgietagung-Veroffentlichungen Berlin-Dresden*, Akademie-Verlag, Berlin, 1953, p 37–49 (in German)
7. G.V. Samsonov, A.D. Panasiuk, M.S. Borovikova et al., *Poroshkovaya Metallurgiya*, 1973, **5**, p 61–67
8. G.A. Yasinskaya, Poroshkovaya Metallurgiya, 1966, **7**, p 53–55 (in Russian)
9. V.N. Achmatov, V.I. Kostikov, and V.F. Melechin, Izvetiya vuzo, *Chernaya Metall.*, 1977, **5**, pp 29–32 (in Russian)
10. G.V. Samsonov, A.D. Panasiuk, and M.S. Borovikova, *Iznosostojkie Naplavochnye Matreialy na Osnovie Tugoplavkich Sojedinienij*, Kiev—Naukova Dumka, 1977, p 63–66 (in Russian)
11. G.V. Samsonov and A.P. Epik, *Tugoplavkie pokrytiya*. Moskva *Metallurgiya*, 1973 (in Russian)
12. L. Xi, I. Kaban, R. Nowak, B. Korpala, G. Bruzda, N. Sobczak, N. Mattern, and J. Eckert, High-Temperature Wetting and Interfacial Interaction Between Liquid Al and TiB₂, *J. Mater. Sci.*, 2015, **50**(7), p 2682–2690
13. A.R. Kennedy and A.E. Karantzalis, The Incorporation of Ceramic Particles in Molten Aluminium and Relationship to the Contact Angle Data, *Mater. Sci. Eng. A*, 1999, **264**, p 122–129
14. N. Sobczak, M. Singh, and R. Asthana, High-Temperature Wettability Measurements in Metal/Ceramic Systems—Some Methodological Issues, *Curr. Opin. Solid State Mater. Sci.*, 2005, **9**(4), p 241–253
15. M.L. Muolo, F. Valenza, N. Sobczak, and A. Passerone, Overview on Wetting and Joining in Transition Metals Diborides, *Adv. Sci. Technol.*, 2010, **64**, p 98–107
16. A. Passerone, M.L. Muolo, R. Novakovic, and D. Passerone, Liquid Metal/Ceramic Interactions in the (Cu, Ag, Au)/ZrB₂ Systems, *J. Eur. Ceram. Soc.*, 2007, **27**(10), p 3277–3285
17. M.L. Muolo, E. Ferrera, R. Novakovic, and A. Passerone, Wettability of Zirconium Diboride Ceramics by Ag, Cu and Their Alloys with Zr, *Scr. Mater.*, 2003, **48**(2), p 191–196
18. N. Sobczak, R. Nowak, A. Passerone, F. Valenza, M.L. Muolo, L. Jaworska, F. Barberis, and M. Capurro, Wetting and Joining of HfB₂ and Ta with Ni, *Prace Instytutu Odlewnictwa*, 2010, **L**(2), p 5–13
19. N. Sobczak, R. Nowak, W. Radziwill, J. Budzioch, and A. Glenz, Experimental Complex for Investigations of High Temperature Capillarity Phenomena, *Mater. Sci. Eng.* 2008, **A495**(1–2), p 43–49
20. L. Liggieri and A. Passerone, *High Temp. Technol.*, 1989, **7**, p 80–86
21. ASTRA Reference Book IENI, Report, 2007
22. N. Eustathopoulos, Progress in Understanding and Modelling Reactive Wetting of Metals on Ceramics, *Curr. Opin. Solid State Mater. Sci.*, 2009, **9**(4), p 152–160
23. T.B. Massalski, H. Okamoto, Eds., Binary Alloy Phase Diagrams, Vol. 1, No. 2, ASM International, Materials Park, 1986
24. N. Sobczak, Wettability and Reactivity Between Molten Aluminum and Selected Oxides, *Solid State Phenom.*, 2005, **101–102**, p 221–226
25. A. Passerone, M.L. Muolo, F. Valenza, F. Monteverde, and N. Sobczak, Wetting and Interfacial Phenomena in Ni–HfB₂ Systems, *Acta Mater.*, 2009, **57**(2), p 356–364
26. F. Valenza, M.L. Muolo, A. Passerone, G. Cacciamani, and C. Artini, Control of Interfacial Reactivity Between ZrB₂ and Ni-Based Brazing Alloys, *J. Mater. Eng. Perform.*, 2012, **21**(5), p 660–666
27. YuV Naidich, V.N. Eremenko, and Z.N. Khim, *Russ. J. Inorg. Chem.*, 1959, **9**, p 2052
28. O. Dezellus, B. Gardiola, and J. Andrieux, On the Solubility of Group IV Elements (Ti, Zr, Hf) in Liquid Aluminium Below 800 °C, *J. Phase Equilib. Diffus.*, 2014, **35**(2), p 120–126
29. H. Duschanek and P. Rogl, The Al-B (Aluminum-Boron) System, *J. Phase Equilib.*, 1994, **15**(5), p 543–544
30. O. Teppo and P. Taskinen, Thermodynamic Assessment of Ni-B Phase Diagram, *Mater. Sci. Technol.*, 1993, **9**(3), p 205–212
31. H. Okamoto and Ni-Zr, *J. Phase Equilib. Diffus.*, 2007, **28**(4), p 409
32. P. Bellen, K. Kumar, and P. Wollants, Thermodynamic Assessment of the Ni-Ti Phase Diagram, *Zeitschrift fur metallkunde*, 1996, **87**(12), p 972–978
33. M. Alzenshtein, N. Froumin, and N. Frage, The Nature of TiB₂ Wetting by Cu and Au, *J. Mater. Eng. Perform*, 2012, **21**, p 655–659
34. S.H. Whang, Y.Q. Gao, and Y.-W. Kim, Age Hardening of Rapidly Quenched Al-Zr-B Alloys, *J. Mater. Sci.*, 1986, **21**(8), p 2839–2842
35. V. Raghavan, Al-B-Ti, *J. Phase Equilib. Diffus.*, 2005, **26**(2), p 173–174